TRANSACTIONS ON EMERGING TELECOMMUNICATIONS TECHNOLOGIES
Trans. Emerging Tel. Tech. (2014)
Published online in Wiley Online Library (wileyonlinelibrary.com). DOI: 10.1002/ett.2871

RESEARCH ARTICLE

Maximum likelihood TOA and OTDOA estimation with first arriving path detection for 3GPP LTE system†

W. Xu[1]*, M. Huang[1], C. Zhu[2] and A. Dammann[3]

[1] Intel Mobile Communications, Am Campeon 10-12, D-85579 Neubiberg, Germany
[2] Technische Universität München, Arcisstr. 21, D-80333 München, Germany
[3] German Aerospace Center (DLR), Institute of Communications and Navigation, Oberpfaffenhofen, D-82234 Wessling, Germany

ABSTRACT

The US Federal Communications Commission (FCC) has mandated wireless network operators and mobile devices to provide accurate location information for E-911. Requirements for time of arrival (TOA) and time difference of arrival (TDOA) measurements have been specified in 3GPP LTE Rel. 9 to ensure accurate user equipment (UE) positioning even under bad conditions (e.g. with channel quickly varying and SNR being as low as −13 dB). To fulfil these requirements, it is vital to accurately estimate the first signal arriving path. In this work, we first derive - without any approximation - the Cramér–Rao lower bound (CRLB) of the LTE TOA and TDOA measurements based on the different pilots, which is shown to be as low as a few metres for $SNR = -13$ dB. The achievable performance of the LTE system is compared with the FCC and 3GPP requirements, and the impact of mobile multipath channels on the measurements is analysed. Then, we describe practical low-complexity methods for LTE TOA and TDOA measurements with enhanced first arriving path detection. The maximum likelihood based correlation profile is used as detection metric. After grossly determining the signal region by a moving window, three methods, namely, peak detection, SNR-based threshold and adaptive threshold based on noise floor and metric peak value are employed to estimate the first arriving path. Simulation results show that the proposed adaptive threshold-based method can meet all 3GPP requirements under various realistic mobile channels, and can in some cases achieve a performance close to the CRLB. Copyright © 2014 John Wiley & Sons, Ltd.

***Correspondence**
W. Xu, Intel Mobile Communications, Am Campeon 10-12, D-85579 Neubiberg, Germany.
E-mail: wen.xu@ieee.org

Received 26 May 2014; Revised 1 August 2014; Accepted 20 August 2014

1. INTRODUCTION

Services and applications based on accurate knowledge of the user position such as location-sensitive billing, fraud detection, fleet management and intelligent transportation systems become increasingly important in recent years. In 1996, the United States Federal Communications Commission (FCC) mandated all US wireless network operators and mobile devices to provide location information for Enhanced-911 (E-911) [1]: Caller location must be provided to public-safety answering points with 50 m accuracy for 67% of calls and 150 m accuracy for 95% of calls. The FCC requirements can be met by global navigation satellite systems such as global positioning system (GPS) in many environments. Typically, the GPS for civil applications can provide a positioning accuracy of a few metres. However, in some environments, such as indoors or in urban canyons, the GPS signal may be too weak to detect or too much scattered to provide required accuracy. As a complement, the wireless communication systems like GSM, UMTS or LTE provide good coverage in such scenarios.

Several methods are available to provide good coverage in GPS critical environment, for example, cell identification (CID), received signal strength, angle of arrival, time of arrival (TOA) and time difference of arrival (TDOA) [2]. In state-of-the-art systems, TDOA-based approaches are usually specified for positioning support [3]. Super resolution TOA estimation methods like MUSIC or ESPIRIT have been employed for indoor TOA and TDOA estimation under middle and low SNR conditions (see, e.g. [4–6]). However, because of the high computational requirements, and the quickly varying channel and very low SNR encountered in mobile communications, the

†Material in this paper was presented in part at the IEEE WCNC' 13 conference, April 2013.

MUSIC or ESPIRIT-based methods may not be suitable for mobile user equipment (UE).

In general, TOA/TDOA estimation can be considered as a special case of channel estimation for which a rich literature exists, for example, [7–16]. Many investigations have been carried out for Ultra Wideband, as well as some multicarrier or OFDM systems, for example, [9–12]. The theoretic framework as well as some suboptimal solutions for TOA/TDOA estimation can, for example, be found in [17] and its references. Some work has also been reported for LTE and LTE-A cellular systems where accurate positioning is one of the key aspects to enable new services and compete with non-cellular systems. For instance, Damman *et al*. [18] investigated the correlation-based method using the secondary synchronisation signals (SSS). As SSS only covers a small bandwidth, its positioning accuracy is limited. Utilising other reference signals or data with higher bandwidth can therefore improve the positioning accuracy. Zhu [19] described a high accuracy synchronisation method for LTE positioning with successive interference cancellation. However, when multipath channel is considered, the decoding error can propagate during the interference cancellation, which will degrade the performance. In [20], the impact of propagation channel for TDOA positioning was studied. Note that in non-line-of-sight (LOS) environments, accurate positioning will become more difficult as the first arriving path (tap) of signal may not be detected. Yang *et al*. [21] proposed a first arriving path detection algorithm using multipath interference cancellation for indoor environments. For outdoor mobile communications, however, the algorithm will become vulnerable to varying channel and very low SNR such that the iterative channel estimation and multipath cancellation become less reliable. In this work, the terms *path* and *tap* are not distinguished from each other, and are interchangeable unless otherwise stated. Observed TDOA (OTDOA) estimation method was also studied during 3GPP LTE standardisation. In [22], an adaptive threshold based on the estimated power of the QPSK-modulated interference signal and the power of the Gaussian noise is computed to detect the OTDOA.

As can be seen, accurate TOA/TDOA estimation is a challenging task in mobile communications. Because of the quickly varying channel and very low SNR, 3GPP has therefore specified the reference signal or pilot called the positioning reference signal (PRS) for LTE system (see next section for details). In this work, we first compute the Cramér-Rao lower bound (CRLB) of the LTE TOA and TDOA measurements based on the different pilots (including PRS), and show the achievable performance limits of the LTE system w.r.t. the FCC and 3GPP requirements. Then, we describe methods for LTE TOA and TDOA measurements with enhanced first arriving path detection. The conventional maximum likelihood (ML) based correlation profile is used as detection metric. After grossly determining the signal region by a moving window, three methods, namely, peak detection, SNR-based threshold and adaptive threshold based on noise floor and metric peak value are employed to estimate the first arriving path. Simulation results show that the proposed adaptive threshold-based method is robust against the quick channel variation and very low SNR, and can meet all 3GPP requirements under AWGN and multipath channels.

The paper is organised as follows. In the next section, we give an overview on the positioning methods standardised for 3GPP LTE. In Section 3, we briefly illustrate the link level model of the LTE signal. Section 4 analyses the TOA and TDOA estimation problems for OFDM signal from theoretical point of view, including deriving the CRLB using different pilots specified for the LTE, showing the achievable performance versus the FCC and 3GPP requirements, and analysing the impact of mobile multipath channels. Detailed description of the proposed practical TOA and TDOA methods for UE receiver is presented in Section 5. Selected simulation results of the proposed methods are given in Section 6, followed by the conclusion in Section 7.

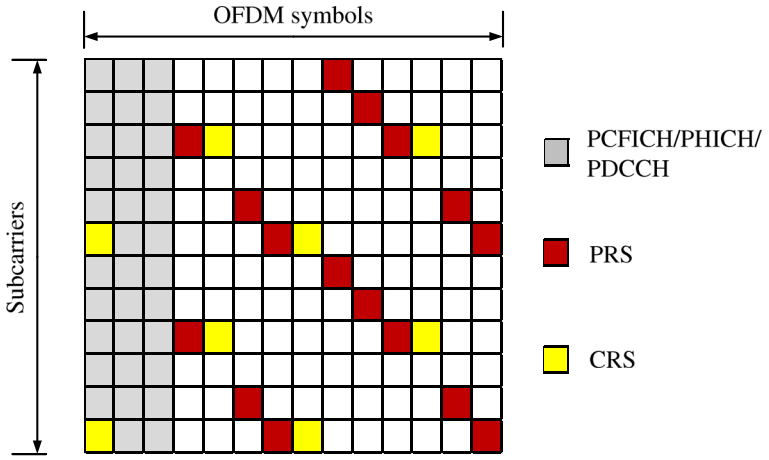

Figure 1. An example LTE signal pattern with cell specific reference signal (CRS) and positioning reference signal (PRS).

2. 3GPP LTE POSITIONING

The LTE standard specifies a set of downlink reference signals with different time-frequency patterns [23, 24], such as those shown in Figure 1. One method for LTE positioning is the enhanced CID (E-CID) [25]. It is a UE-assisted and network-based method that utilises cell IDs, RF measurements from multiple cells, TOA, and angle of arrival measurements. Cell specific reference signal (CRS) is commonly used for the E-CID measurement.

Another UE-assisted method called the OTDOA has attracted more attention for providing high accuracy. In 3GPP LTE Rel. 9, the PRS is introduced to enhance the positioning measurements in combination with low interference subframes, to ensure sufficiently high signal quality and detection probability. The PRS is distributed in time and frequency in the so-called positioning occasion, which allocates consecutive positioning subframes with a certain periodicity. When the PRS is present, no data but only control signalling are transmitted, which greatly reduces the neighbour cells interference. The sophistication of this signal is even higher when the network mutes the PRS transmissions of certain base stations (i.e. PRS muting), in order to further reduce the inter-cell interference. When PRS is not available, CRS can be used to estimate the OTDOA. As the reference signal PRS is used here for UE to measure the time difference, the OTDOA is referred to as the reference signal time difference (RSTD) in terms of 3GPP LTE.

Similarly, for E-CID, the so-called UE Rx–Tx time difference is measured. The UE Rx–Tx time difference is defined as the difference between the UE received (Rx) timing of the downlink radio frame and the UE transmit (Tx) timing of the uplink radio frame [26]. Consider that the Tx timing is known at the UE, the Rx–Tx time difference measurement is dependent only on the RX timing. Consequently, it is a TOA measurement, although it represents a time difference. In this work, we may therefore use TOA and Rx–Tx time difference, as well as OTDOA and RSTD, interchangeably

3. SIGNAL MODEL

In time domain, the n-th sample in l-th OFDM symbol can be expressed as

$$x_l(n), n \in [-G, N-1], l \in [0, N_{symb}-1] \tag{1}$$

where G is the length of cyclic prefix (CP), N is the size of FFT, and N_{symb} is the number of OFDM symbols (e.g. within a subframe). The CP is the duplicate of the last G samples of the OFDM symbol, $x_l(n) = x_l(n+N), n \in [-G, -1]$.

We denote the channel impulse response of the mobile multipath channel as $h_l(0), \ldots, h_l(N-1)$, where the channel tap has a distribution $h_l(i) \sim \mathcal{CN}(\mu_l(i), \gamma_l(i))$. $\mu_l(i)$ and $\gamma_l(i)$ are the mean and power of the i-th tap ($\gamma_l(i) = 0$ for $i \geqslant L$), respectively. Then, the received signal $y_l(n)$ can be expressed as

$$y_l(n) = \sum_{i=0}^{L-1} h_l(i) x_l(n-i-\tau) + z_l(n) \tag{2}$$

$$n \in [-G, N+L+\tau-1] \tag{3}$$

where τ is the propagation delay of the signal, the parameter related to the TOA, and $z_l(n) \sim \mathcal{CN}(0, \sigma^2)$ is the additive complex Gaussian noise.

4. THEORETICAL ANALYSIS

Maximum likelihood estimator is optimal in the sense of the likelihood of the estimated parameters. With the aid of pilots or reference signals, the starting point of the received signal can be detected by ML estimator to further estimate TOA. The theoretical accuracy of the TOA estimation is limited by the CRLB. In this section, we compute the CRLB of TOA estimation for the OFDM-based LTE signal. Here, we relax the constraint of the TOA τ to positive real number (instead of integer multiplication of the sampling time interval T_s). With the pilot signal s_l, the signal model in Equation (2) can be revised to

$$y_l(nT_s) = \int_{\nu=0}^{LT_s} h_l(\nu) s_l(nT_s - \tau - \nu) d\nu + z_l(nT_s) \tag{4}$$

4.1. CRLB and achievable TOA/TDOA limits

A. CRLB of TOA estimation under AWGN

For any parameter ζ, the CRLB of the estimate $\hat{\zeta}$ based on the observation vector y can in general be expressed as

$$\mathrm{var}\{\hat{\zeta}(y)\} \geqslant \frac{\left\| \frac{\partial}{\partial \zeta} E\{\hat{\zeta}(y)\} \right\|^2}{E\left\{ \left\| \frac{\partial}{\partial \zeta} \ln\left(p(y|\zeta)\right) \right\|^2 \right\}} := \mathrm{CRLB}(\zeta) \tag{5}$$

For static AWGN channel, we have $h_l(0) = 1$ and $h_l(t) = 0$ for $t \neq 0$. It is well-known that the CRLB of the TOA τ using an unbiassed ML estimator can be expressed as (see, e.g. [27–31])

$$\mathrm{var}\{\hat{\tau}\} \geqslant \frac{\sigma^2}{2 \sum_{l=0}^{N_{symb}-1} \sum_{n=0}^{N-1} \left| \frac{\partial}{\partial \tau} s_l(nT_s - \tau) \right|^2} \tag{6}$$

where σ^2 is the complex noise power defined earlier and a total of $N_{symb}N$ time samples observations are used. If we denote the subcarrier spacing in frequency domain

by $\Delta f = 1/(NT_s)$, then for the l-th OFDM symbol, the baseband signal $s_l(nT_s - \tau)$ can be written as

$$s_l(nT_s - \tau) = \frac{1}{\sqrt{N}} \sum_{k=-N/2}^{N/2-1} S_l(k)\, \mathrm{e}^{j2\pi k \Delta f (nT_s - \tau)} \tag{7}$$

where $S_l(k)$ is the signal allocated on the k-th subcarrier of the l-th OFDM symbol. Because only the subcarriers of the reference signals are effective in ML estimation, we can assume $S_l(k_d) = 0$ for k_d being the subcarrier indices of non-reference signals.

To obtain the CRLB by Equation (6), we calculate the norm of the derivative

$$\begin{aligned} \left| \frac{\partial}{\partial \tau} s_l(nT_s - \tau) \right|^2 &= \left| \frac{\partial}{\partial \tau} \frac{1}{\sqrt{N}} \sum_k S_l(k) \mathrm{e}^{j2\pi k \Delta f (nT_s - \tau)} \right|^2 \\ &= \frac{4\pi^2 \Delta f^2}{N} \sum_k \sum_m mk S_l^*(m) S_l(k) \\ &\cdot \mathrm{e}^{j\frac{2\pi}{N}(k-m)n} \mathrm{e}^{j2\pi \Delta f (m-k)\tau} \end{aligned} \tag{8}$$

For simplicity, we have ignored the summation range of subcarrier indices k and m in Equation (8). Here, the subcarrier index is assumed from $-N/2$ to $N/2 - 1$ when no additional note is provided. For the $N_{symb}N$ available time-domain samples, we have

$$\begin{aligned} &\sum_{l=0}^{N_{symb}-1} \sum_{n=0}^{N-1} \left| \frac{\partial}{\partial \tau} s_l(nT_s - \tau) \right|^2 \\ &= \frac{4\pi^2 \Delta f^2}{N} \sum_k \sum_m mk \sum_{l=0}^{N_{symb}-1} S_l^*(m) S_l(k) \mathrm{e}^{j2\pi \Delta f (m-k)\tau} \\ &\cdot \underbrace{\sum_{n=0}^{N-1} \mathrm{e}^{j\frac{2\pi}{N}(k-m)n}}_{=N\delta_{mk}} \end{aligned} \tag{9}$$

where δ_{mk} is the Kronecker delta function defined as

$$\delta_{mk} = \begin{cases} 1 & \text{if} \quad m = k, \\ 0 & \text{otherwise} \end{cases} \tag{10}$$

Consequently, the CRLB of the TOA estimation for AWGN can be obtained by

$$\mathrm{var}\{\hat{\tau}\} \geqslant \mathrm{CRLB}(\hat{\tau}) = \frac{\sigma^2}{8\pi^2 \Delta f^2 \sum_{l=0}^{N_{symb}-1} \sum_{k=-N/2}^{N/2-1} k^2 |S_l(k)|^2} \tag{11}$$

It should be noticed that results *similar* to (11) based on *continuous* Fourier transform do exist, for example, in [11, 17, 28], where the mathematical derivation of the CRLB has in turn been referred to [27]. In [27] (p. 55), the CRLB was derived by assuming the sampling interval to be small enough to approximate the sum by an integral. In [28], an approximation of the modified CRLB for time-delay estimation as a function of the spectral properties of a modulated signal was given. Del Peral-Rosado *et al.* [31] employed the result of Kay [27] to obtain the CRLB given in (11) through approximating the mean square bandwidth by considering a rectangular power spectral density. In this study, the CRLB (11) has been derived rigorously by directly using *discrete* Fourier transform. Neither the sampling interval approaching to zero nor the mean square bandwidth approximation is required. This—to authors knowledge—has not yet been reported by others. Note that the sampling interval of the LTE baseband signal is equal to $16T_s$, $8T_s$, $4T_s$, …, T_s for the LTE bandwidth 1.4, 3, 5, …, 20 MHz, respectively, and may not be considered to approach zero, where T_s = 1/30.72 μs = 32.552 ns is the *basic (time) unit* for LTE (Section 6).

As expected, the accuracy (in terms of CRLB) of the timing estimation in OFDM system depends on the allocated signal power. If the total signal power for transmitting an OFDM symbol is constant, the estimation accuracy is increased when more power is allocated to the higher frequency subcarriers.

B. Achievable TOA/TDOA measurement accuracy under AWGN using different pilots in LTE

Figures 2, 3 and 4 show the CRLBs of timing estimation, namely $\sigma_{CRLB} := \sqrt{CRLB(\hat{\tau})}$, computed according to (11) using different pilots specified in 3GPP LTE and one receive antenna, with $E_s := E\{|S_l(k)|^2\}$ being constant for the pilots specified in LTE system, such as the primary synchronisation signal (PSS), SSS, CRS and PRS. The left y-axis of the diagrams is scaled in seconds [s], and the right y-axis has a scaling unit of three metres [3 m] in terms of pseudo-range by assuming a radio wave transmits at 0.3×10^9 m/s. Here, a subframe of 1 ms contains 14 consecutive OFDM symbols, as in the case of the LTE normal CP. Four sorts of pilots including PSS, SSS, CRS and PRS are mapped to the corresponding resource elements [23].

In the figures, the lowest bound (i.e. the highest measurement accuracy) is obtained by utilising *all* the four pilots (PSS/SSS, CRS and PRS) simultaneously. Among all available pilots in LTE, the PRS, as expected, achieves the highest accuracy in terms of the CRLB because it almost spans the whole bandwidth and there are also more PRS symbols available than, say, CRS symbols (e.g. see Figure 1).

As can be seen, using the PRS instead of the CRS can in general have a gain of about 3 dB. When CRS in addition to PRS is used, about one extra decibel can be gained.

It should be noted that the CRLB σ_{CRLB} shown in Figures 2–4 represents the standard deviation of the TOA measurements (or measurement errors) in seconds for ideal AWGN channel. When TDOA, the difference of TOA, is considered, and the two measurements are independent and have the accuracy, say, $\sigma_{1,CRLB}$ and $\sigma_{2,CRLB}$, then the standard deviation of the corresponding CRLB for TDOA will become $\sqrt{\sigma_{1,CRLB}^2 + \sigma_{2,CRLB}^2}$.

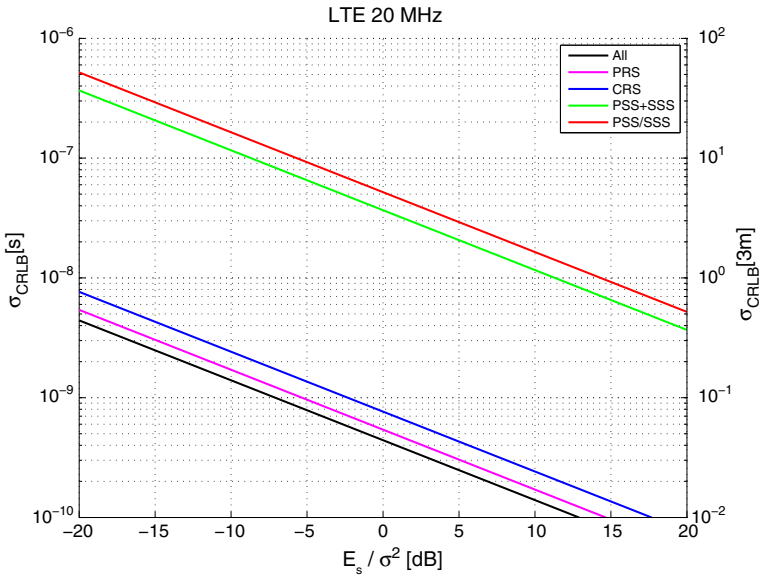

Figure 2. CRLB in seconds and in 3 m for TOA measurement using different pilots in one subframe (20 MHz LTE).

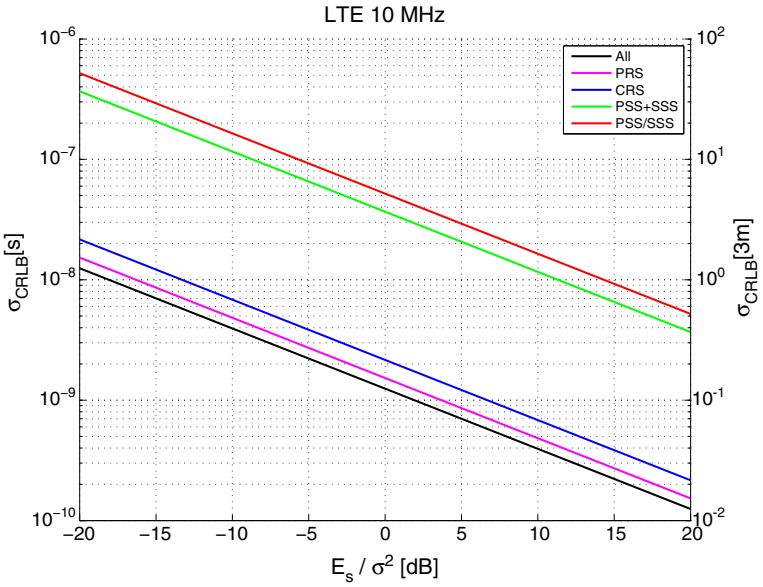

Figure 3. CRLB in seconds and in 3 m for TOA measurement using different pilots in one subframe (10 MHz LTE).

Assume the measurements have a Gaussian distribution, then statistically about two-third (68%) of the measurements would be distributed within one standard deviation from the mean, which is σ_{CRLB} for TOA, and $\sqrt{\sigma^2_{1,CRLB} + \sigma^2_{2,CRLB}}$ for TDOA, respectively. In other words, Figures 2–4 show the accuracy of the TOA measurements with the confidence level of 68%. When 90% confidence level is applied, as in the case of 3GPP, the corresponding CRLB for TOA and TDOA measurements become $\sigma_{CRLB,90\%} = 1.64 \times \sigma_{CRLB}$ and $\sigma_{CRLB,90\%} = 1.64 \times \sqrt{\sigma^2_{1,CRLB} + \sigma^2_{2,CRLB}}$, respectively.

Now consider the cases for the TDOA where the pilot signals from the two base stations received at UE having SNR $= -13$ dB.

(1) *Using PRS alone:* Note that both PRS and CRS almost span the whole signal bandwidth. As shown in Figure 2, the TDOA measurement accuracy for 20 MHz system at the confidence level 68% equals $\sqrt{2}\sigma_{CRLB}|_{PRS,20MHz} = \sqrt{2} \times 2.4 \times 10^{-9}$ s $= 3.4$ ns, which corresponds to about 1 m. Similarly, we have for 10 MHz system, $\sqrt{2}\sigma_{CRLB}|_{PRS,10MHz} = \sqrt{2} \times 6.8 \times 10^{-9}$ s $= 10$ ns $\hat{=}$ 3 m (cf. Figure 3).

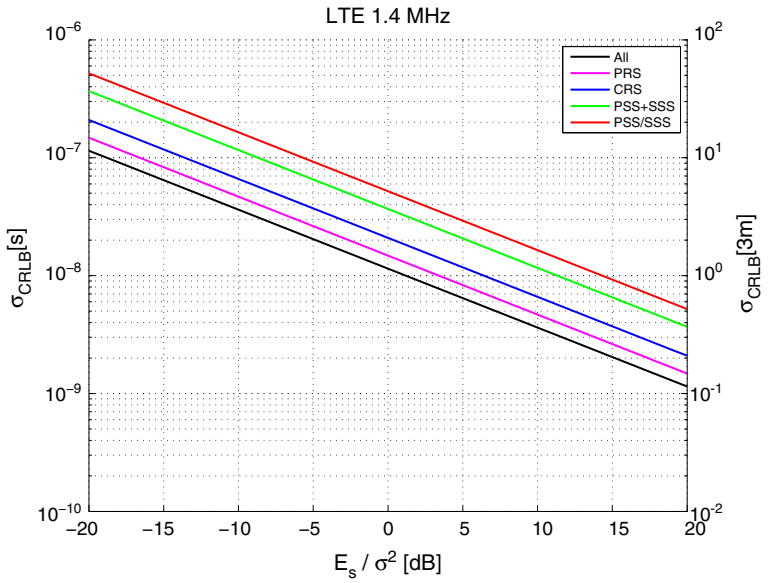

Figure 4. CRLB in seconds and in 3 m for TOA measurement using different pilots in six subframes (1.4 MHz LTE).

(2) *Using PSS and SSS:* Both PSS and SSS transmit every 5 ms and occupy 62 subcarriers. Thus, they have a fixed bandwidth of $62 \times \Delta f = 936$ kHz, irrespective of the LTE system bandwidth. When using one PSS and one SSS, we have $\sqrt{2}\sigma_{CRLB}|_{PSS+SSS} = \sqrt{2} \times 1.64 \times 10^{-7}$ s $= 232$ ns $\hat{=}$ 70 m, which does not fulfil the FCC requirement of 50 m accuracy for 67% of calls.

(3) *LTE 1.4 MHZ bandwidth:* This lowest bandwidth is apparently a critical scenario for the LTE positioning. Therefore, six subframes of data (pilots) are typically employed for the 1.4 MHz case, as recommended by 3GPP. The corresponding CRLB is shown in Figure 4. In this case, when all available pilots (PRS, CRS, PSS and SSS) are used, we have $\sqrt{2}\sigma_{CRLB}|_{All,1.4MHz} = \sqrt{2} \times 51 \times 10^{-9}$ s $= 72$ ns $\hat{=}$ 22 m. When only PRS, or CRS is used, we obtain $\sqrt{2}\sigma_{CRLB}|_{PRS,1.4MHz} = \sqrt{2} \times 66 \times 10^{-9}$ s $= 93$ ns $\hat{=}$ 28 m, or $\sqrt{2}\sigma_{CRLB}|_{CRS,1.4MHz} = \sqrt{2} \times 93 \times 10^{-9}$ s $= 132$ ns $\hat{=}$ 40 m, respectively.

We can verify other LTE pilots shown in Figures 2–4. As a result, we see that when CRS and/or PRS is used, the best TDOA estimate achieving the CRLB can fulfil the FCC requirement of 50 m accuracy for 67% of calls, even for the lowest LTE bandwidth 1.4 MHz (where six subframes are used). When more time/measurement data is available, say for slowly varying channel, still higher accuracy can be achieved.

C. Achievable TOA/TDOA measurement accuracy under mobile multipath channel

For a static multipath channel, that is, $h_l(i)$ in Equation (2) is not time-varying, the CRLB can also be derived by jointly estimating all channel paths. Specifically, the CRLB of the first path timing estimate will become *independent* of other paths when the other paths are resolvable from the first one. Otherwise, it will be no less than that of the single path timing estimate, as, for example, shown in [9, 12, 17, 32]. We will analyse in the following how the other paths impact the first path timing estimation, also when the channel is not static.

The mobile channel dealt with in this study (such as ETU3—Extended Typical Urban model with maximum Doppler frequency of 3 Hz, EPA5—Extended Pedestrian A model with maximum Doppler frequency of 5 Hz, etc.) has usually multipaths and is unfortunately not static. The channel taps are random variables, for example, generated according to the Jakes spectrum employed in 3GPP channel models [33], and varying with time. Therefore, there exists theoretically no CRLB for estimating these channel taps. Obviously, the accuracy limit by the CRLB for a static multipath channel can usually not be achieved in the case of a mobile multipath channel, and the CRLB for the static AWGN channel (as shown earlier) in turn cannot be achieved by that of a static multipath channel. In other words, the CRLB of TOA/TDOA estimation for AWGN can serve as an accuracy limit, which any TOA/TDOA estimate under any channel cannot exceed.

A rigorous theoretical analysis on the performance gaps among AWGN, the static and the mobile multipath channels are beyond the scope of this study. Instead, we will show in next sections the performances of the proposed practical algorithms under AWGN and the 3GPP mobile multipath channels, compared with the CRLB for the static AWGN channel.

4.2. Impact of mobile multipath channel on TOA estimation

For a static channel, it is well-known that under some regularity conditions (i.e. the derivatives of the log-likelihood function exist and the Fisher information is nonzero), the ML estimator is asymptotically unbiassed and attains the CRLB [27]. In [34], a closed-form expression of the CRLB for range estimation in multicarrier systems was derived in the presence of interference, where static channel taps were assumed. Contrary to the conventional system model using the AWGN alone as the total interference-plus-noise, the sum of two terms, namely, an AWGN term and a stationary interference term with given power spectral density, was used as the total interference-plus-noise.

For either static or mobile channel, the ML estimate of the delay of the first arriving path τ_0 can be carried out by searching for the correlation peak. In the following, we will show that this will lead to a biassed estimate when multipath is present. To analyse the bias, we rewrite Equation (2) for continuous time instant t as

$$y_l(t) = h_0 x_l(t-\tau_0) + \sum_{i=1}^{L-1} h_i x_l(t-\tau_0-\Delta_i) + z(t) \quad (12)$$

For simplicity, we assume the random variables h_i and z are independent and ergodic. For OFDM, the signal $x_l(t)$ can be separated into pilot part $s_l(t)$ and data part $d_l(t)$ as $x_l(t) = s_l(t) + d_l(t)$. Assume they are uncorrelated pseudo noise sequences, such as those specified in LTE, and fulfil $E\{d_l(t)s_l^*(t)\} = \int_{-\infty}^{+\infty} d_l(t)s_l^*(t)dt = 0$, and $E\{z(t)s_l^*(t-\tau)\} = 0$. Then, by denoting $R_0(\tau) := E\{s_l(t)s_l^*(t-\tau)\}$, we have

$$\begin{aligned} R(\tau) &= E\{y_l(t)s_l^*(t-\tau)\} \\ &= \mu_0 R_0(\tau-\tau_0) + \sum_{i=1}^{L-1} \mu_i R_0(\tau-\tau_0-\Delta_i) \end{aligned} \quad (13)$$

Assume that the phase of the first arriving path $\varphi = \dfrac{\mu_0}{|\mu_0|}$ can be estimated, a coherent estimator can then be constructed as

$$\hat{\tau} = \arg\max_{\tau} \Re\{\varphi^* R(\tau)\} \quad (14)$$

where $\Re\{\cdot\}$ denotes the real part of the number. According to Equation (13), the function $\tilde{\psi}(\tau) := \Re\{\varphi^* R(\tau)\}$ can be expressed as

$$\begin{aligned} \tilde{\psi}(\tau) &= \Re\{|\mu_0| R_0(\tau-\tau_0)\} \\ &\quad + \sum_{i=1}^{L-1} \Re\left\{\varphi^* \mu_i R_0(\tau-\tau_0-\Delta_i)\right\} \end{aligned} \quad (15)$$

We further denote

$$\begin{aligned} g_0(\tau) &= |\mu_0| \Re\{R_0(\tau-\tau_0)\} \\ g_i(\tau) &= \Re\left\{\hat{\varphi}^* \mu_i R_0(\tau-\tau_0-\Delta_i)\right\} \end{aligned} \quad (16)$$

then, we have

$$\tilde{\psi}(\tau) = \sum_{i=0}^{L-1} g_i(\tau) \quad (17)$$

Assume the biassed estimate $\hat{\tau}$ is close to the exact value τ_0, we can approach the functions $g_i(\tau)$ with the second order Taylor expansion at point τ_0 for $i = 0, \ldots, L-1$

$$g_i(\tau) = g_i(\tau_0) + g_i'(\tau_0)(\tau-\tau_0) + \frac{1}{2} g_i''(\tau_0)(\tau-\tau_0)^2 \quad (18)$$

Thus, the timing $\hat{\tau}$ estimated by the coherent estimator fulfils

$$\frac{d}{d\tau}\tilde{\psi}(\tau) = \sum_{i=0}^{L-1} \left(g_i'(\tau_0) + g_i''(\tau_0)(\tau-\tau_0)\right) = 0 \quad (19)$$

Because the real part of the autocorrelation function R_0 achieves its maximum at 0, i.e. $\Re\{R_0'(0)\} = 0$, we have $g_0'(\tau_0) = 0$. Therefore, the total bias of the correlation-based ML timing estimation caused by $L-1$ delayed paths is approximately

$$\hat{b}_\tau = \hat{\tau} - \tau_0 = -\frac{\sum_{i=1}^{L-1} g_i'(\tau_0)}{\sum_{i=0}^{L-1} g_i''(\tau_0)} \quad (20)$$

As expected, for single path channel, we have $g_i'(\tau) = 0$ for $i > 0$ such that the estimate $\hat{\tau}$ is unbiassed (i.e. $\hat{b}_\tau = 0$). Intuitively, more power in delayed paths results in a larger bias. The bias can be approximated by Equation (20) if the power, delay and phase shift of all the signal paths are available.

When the power, delay and phase shift of the signal paths cannot be reliably estimated, as usually in the case of mobile communications, a non-coherent estimator (as shown in next section) can be employed, where the TOA is obtained by

$$\hat{\tau} = \arg\max_{\tau} |R(\tau)|^2 \quad (21)$$

Similarly, the estimation is also biassed when there are more than one path. The bias will become complex especially under a mobile multipath channel where the channel is varying. Notice that the performance of channel estimation usually relies on an accurate timing estimation, so error may propagate if the TOA estimate is not adequately precise. As a feasible solution, we propose practical TOA estimators based on first tap detection and show their reliable performances in the following sections.

5. PRACTICAL TOA ESTIMATION BASED ON FIRST TAP DETECTION

5.1. Maximum likelihood timing estimation

The reference signal $s_l(n)$, such as CRS and/or PRS, is embedded in the received signal $y_l(n)$. The target of the TOA estimation is to determine the position τ in the received signal y_l, say, using the ML criterion. Notice that the ML estimator has the asymptotic properties of being unbiassed and achieving the CRLB [27]. Consider the other paths as interference, the ML criterion for timing estimation of the first path reduces to a correlation-based criterion (see, e.g. [35]). The correlation-based method can be realised in time or frequency domain. In the following, we focus on the time-domain-based method.

The received signal $y_l(n)$ is correlated with the replica of the transmitted signal $s_l(n)$, that is,

$$R(t) := \sum_{l=0}^{N_{symb}-1} \sum_{n=0}^{N-1} y_l(n+t) s_l^*(n), t = [0, W-1] \quad (22)$$

where $W = 2G$ is chosen as the search window size. To ease the analysis, we first assume $s_l(n)$ has ideal autocorrelation property, and the power of the transmit signal $s_l(n)$ is P_s. Then, with some derivations, the correlation can be written as

$$R(t) = P_s \sum\nolimits_{l=0}^{N_{symb}-1} h_l(t-\tau) + R_{res}(t) \quad (23)$$

where $R_{res}(t)$ represents the total residual noise and interference part resulting from correlation between $s_l(n)$ and $z_l(n+t)$.

Assume that the channel is unknown but remains invariant for N_{symb} OFDM symbols, $h_l(t) = h(t)$, then the non-coherent detector can be employed. The metric for the TOA detection, which is also called the *correlation profile*, is given here by

$$\begin{aligned} \Lambda(t) &:= E\{|R(t)|^2\} \\ &= E\left\{(N_{symb} P_s |h(t-\tau)|)^2\right\} + P_s N_{symb} \sigma^2 \\ &= N_{symb}^2 P_s^2 \gamma(t-\tau) + P_s N_{symb} \sigma^2 \end{aligned} \quad (24)$$

with $\gamma(t) := E\{|h(t)|^2\}$. $E\{|R(t)|^2\}$ is used to denote the statistical average of $|R(t)|^2$ over multiple subframes containing RS signals. In the LTE, a group of several consecutive subframes containing the RS is sometimes referred to as a positioning occasion (Section 6.1). Usually, an LTE positioning measurement is performed with one or more occasions. In our study, the statistical average is implemented as arithmetic mean over multiple subframes. As the channel h may vary significantly from subframe to subframe, the average of $|R(t)|^2$, instead of $R(t)$, is employed here to ensure that channel power delay profile is preserved in the resulting metric $\Lambda(t)$.

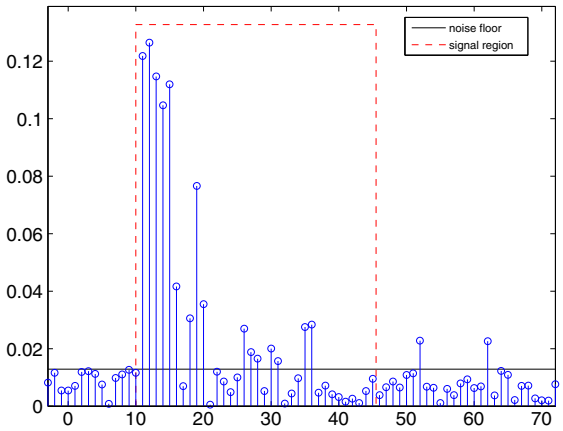

Figure 5. An example correlation profile $\Lambda(t)$.

5.2. Signal arrival region determination

The next step in our method for TOA measurement is to determine the arrival region of the reference signal in the whole search window. For a multipath channel, the signal arrival region will have multiple taps corresponding to the taps of the channel (Figure 5). The signal paths are therefore reflected by the channel paths. A moving sum for the window size of CP length is then computed

$$\Lambda_{win}(u) = \sum_{t=u}^{u+G-1} E\{|R(t)|^2\}, u \in [0, G-1] \quad (25)$$

The signal can be regarded as arrived in the time region

$$\begin{aligned} & u_0 \leqslant t \leqslant u_0 + G - 1 \\ s.t. \quad & u_0 = \arg\max_u \{\Lambda_{win}(u)\} \end{aligned} \quad (26)$$

When $t - \tau \geqslant L$ or $t - \tau < 0$, only the noise power related term, called here the noise floor, $N_f := P_s N_{symb} \sigma^2$, remains in the correlation. The noise floor N_f can be calculated by averaging the terms outside the signal region. As confirmed in our study, such a moving window can reliably detect the signal region, which can effectively eliminate big detection errors (outliers) often occurring in the next step, the first path (tap) detection. In the proposed algorithms, N_f instead of σ^2 is used.

5.3. SNR-based first tap detection

Determining the signal arrival time, that is, the TOA τ, is a classic signal detection problem. For a single path channel, such as in the case of the LOS signal, the TOA can be detected, by searching for the path with the strongest signal power. For a multipath channel, in particular when the first arriving path is not the strongest (e.g. under ETU channel), the TOA estimation becomes biassed. Usually, a threshold is needed to determine the first arriving path. Especially

in the case of strong noise and interference from multiple cells, the metric $\Lambda(t)$ may not provide sufficient accuracy. For this reason, an SNR-based metric is given here.

Consider

$$\frac{E\left\{|R(t)|^2\right\}}{N_f} = \frac{N_{symb}P_s\gamma(t-\tau)}{\sigma^2} + 1 = N_{symb}SNR(t) + 1 \quad (27)$$

where $SNR(t) := \frac{P_s\gamma(t-\tau)}{\sigma^2}$ is the SNR for each correlation sample, and it holds

$$SNR(t) = \frac{1}{N_{symb}}\left(\frac{E\{|R(t)|^2\}}{N_f} - 1\right) \quad (28)$$

The following criterion then takes a fixed SNR value as threshold to estimate the first tap

$$\tau = \min_{u_0 \leqslant t < u_0+G-1}\{t\} \quad s.t.\ SNR(t) \geqslant SNR_{th} \quad (29)$$

SNR_{th} is the required SNR for detection, which can be set as, for example, −13 dB for 3GPP Rel. 9 OTDOA measurement.

5.4. Adaptive threshold-based first tap detection

As $s_l(n)$ is not ideally autocorrelated, the noise floor N_f would contain further terms besides $P_sN_{symb}\sigma^2$. Therefore, we can express the noise floor as

$$N_f = P_sN_{symb}\sigma^2 + \varepsilon(N_{symb}) \quad (30)$$

where $\varepsilon(N_{symb})$ is a parameter related to N_{symb}, $s_l(n)$ and $y_l(n)$, and $y_l(n)$ is in turn dependent on the channel and the interference. When only a few OFDM symbols are considered for averaging or the interference is strong, $\varepsilon(N_{symb})$ will be more significant than the noise floor term. Thus, the estimated $SNR(t)$ value would be smaller than the actual one. When the first arriving path contains too small power, it may not be able to detect.

For this reason, another criterion is proposed here. This criterion jointly considers the noise power and the received *signal* power to determine a varying (adaptive) detection threshold. Assume the metric peak relying on the signal power and noise is (Figure 5)

$$\Lambda_{max} = \max_{u_0 \leqslant t < u_0+G-1}\left\{E\left\{|R(t)|^2\right\}\right\} \quad (31)$$

The adaptive threshold can then be defined as

$$\Lambda_{th} = \alpha\sqrt{\Lambda_{max}N_f} \quad (32)$$

Alternatively, the threshold can be defined as

$$\Lambda_{th} = \alpha(\beta\Lambda_{max} + (1-\beta)N_f) \quad (33)$$

where α is a design parameter, $\beta \in [0, 1]$ is a constant trading off between the noise floor and the metric peak. α and β were determined through simulations, to have a trade-off for different channels and different SNRs. For all simulation results presented in next sections, the fixed parameters $\alpha = 1$, $\beta = 0.5$ were used, which were found to be robust for different scenarios. As the performances using (32) and (33) were similar, only the results using (32) are presented in this study.

Given the threshold, the criterion for the adaptive threshold detection can be expressed as

$$\tau = \min_{u_0 \leqslant t < u_0+G-1}\{t\} \quad s.t.\ E\{|R(t)|^2\} \geqslant \Lambda_{th} \quad (34)$$

As can be seen in next section, this criterion leads to better performance especially under a multipath channel.

5.5. Estimated TOA refinement

For $s_l(n)$ is not ideally autocorrelated, especially for coherent accumulation, the correlation function has side-lobes at both sides, before and after the main lobe. Using the threshold may detect the side lobe before the main lobe as the first arriving path. Specifically, when the *actual* main lobe of the first arriving path lies between two samples, it may be difficult to tell whether the detected tap is the actual first tap or the side lobe.

To reduce the deviation caused by the side lobe, smoothing average for the detected tap and its neighbouring taps is performed as the next step, for example, over three taps,

$$\tau' = \frac{\sum_{t=\tau-1}^{\tau+1} t\Lambda(t)}{\sum_{t=\tau-1}^{\tau+1}\Lambda(t)} \quad (35)$$

The smoothing over some neighbouring taps is reasonable, as $R(t)$ is band-limited. According to Nyquist sampling theorem, it can be expressed as an interpolation of discrete samples, for example,

$$E'\{|R(t)|^2\} = \sum_{i=-\infty}^{\infty} E\{|R(i)|^2\}w(t-i) \quad (36)$$

with $w(i) = \frac{\sin(i)}{i}$. When some samples are missing or distorted by interference and noise, they can be restored by smoothing.

From Figure 6, we can see that, when threshold is set too low, the side lobe is detected as first arriving path. However, with the smoothing, the final estimated first arriving path tends to approach the actual one. When threshold is set too high, the actual first arriving path may also be missing.

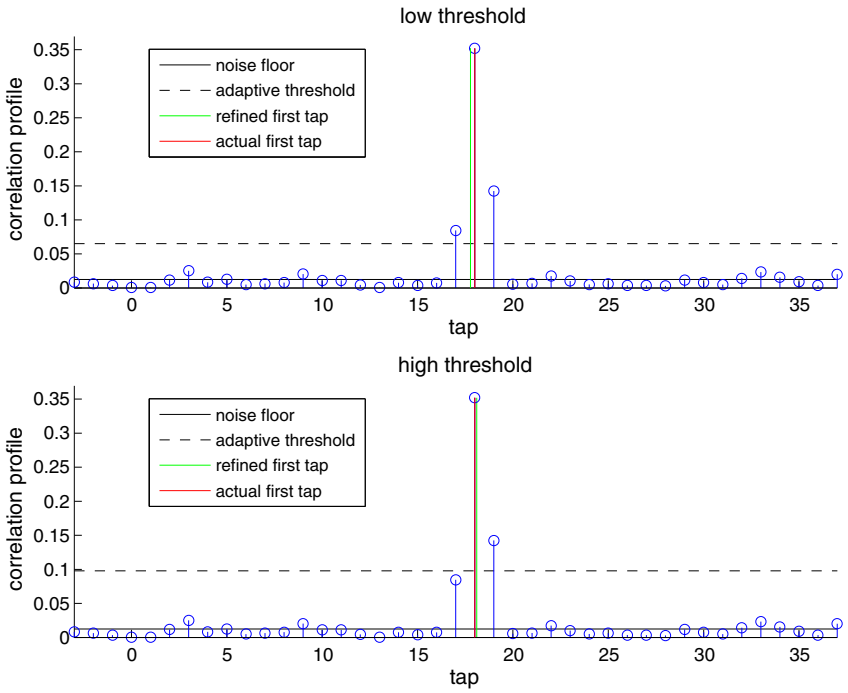

Figure 6. First tap detection with lower and higher threshold.

Through the averaging over the neighbouring taps, the first arriving path can be more accurately found.

After estimating the TOA for different cells, the TDOA or OTDOA can be calculated as

$$\Delta\tau_{ij} = \tau_i' - \tau_j' \tag{37}$$

where τ_i' and τ_j' denote the estimated TOA for cell i and cell j, respectively.

5.6. Enhancement in low bandwidth

The Rel. 8/9 LTE supports bandwidths up to 20 MHz, which corresponds to a sampling rate of 30.72×10^6 samples/s in baseband signal. For bandwidth smaller than 20 MHz, decimation is usually carried out in baseband in order to reduce the following processing load. For example, when the system has a bandwidth of 1.4 MHz, the baseband signal can be obtained by 16 times down-sampling of the 20 MHz signal. Note that the following processing can also be carried out without down-sampling when only the signal within the actual bandwidth is considered. In other words, direct processing of a 1.4 MHz signal with a sampling rate of 30.72×10^6 samples/s corresponds to an oversampling of the 1.4 MHz signal by a factor 16. Although the effective bandwidth remains unchanged, better results can be obtained in the case of oversampling because of the receive diversity gain.

Note that the same TOA/TDOA measurement accuracy requirements are defined for 10, 15 and 20 MHz LTE systems. In our simulations shown in the next section, the 10 MHz baseband signal with a sampling rate of 15.36×10^6 samples/s was used to estimate the RSTD and Rx–Tx time difference for the 1.4–20 MHz LTE system. The corresponding FFT/IFFT size is 1024. The sampling rate 15.36×10^6 samples/s provides a good trade-off between computational complexity and performance. In addition, the same accuracy requirement has been standardised for 10, 15 and 20 MHz LTE. When still higher sampling rate is used (e.g. 30.72×10^6 samples/s), slightly better performances can be obtained.

5.7. Implementation complexity

The main complexity of the investigated TOA (i.e. Rx–Tx time difference) or OTDOA (i.e. RSTD) methods lies on computing the correlation profile. The other steps, such as the signal arrival region determination, adaptive threshold determination and TOA refinement, can be realised with low computational efforts. For a 10 MHz system, as used in our example implementation, maximally 10 OFDM symbols with CP are used for correlation, which amounts to 10 968 samples. With a searching window of $2G$, approximately 1.5×10^6 complex multiplications are needed for one positioning occasion. This amount of computations can be carried out by currently available modem DSPs. Alternately, the correlation can also be realised in frequency domain, by employing efficient FFT/IFFT.

6. SIMULATION RESULTS

6.1. Simulation setup

For RSTD and Rx–Tx time difference measurements, different accuracy requirements are defined for different system bandwidths [36]. 3GPP LTE requires 15 and 5 T_s RSTD measurement accuracy for 1.4 and 10 MHz, respectively. 20 T_s / 10 T_s are required for Rx–Tx time difference measurement for bandwidth smaller than or equal to/larger than 3 MHz (see Tables I and II). $T_s = 32.552$ ns is the *basic unit* defined in 3GPP LTE, which corresponds to 9.77 m in pseudo-range measurement.

Table I. 3GPP LTE RSTD measurement requirements [36].

Bandwidth	N_{PRS}	Accuracy (T_s)	Accuracy (m)
$\leqslant$ 3 MHz	6	$\pm$15	$\pm$146.6
= 5 MHz	2	$\pm$6	$\pm$58.6
$\geqslant$ 10 MHz	1	$\pm$5	$\pm$48.9

Table II. 3GPP LTE Rx–Tx time difference measurement requirements [36].

Bandwidth	Accuracy (T_s)	Accuracy (m)
$\leqslant$ 3 MHz	$\pm$20	$\pm$195.4
$\geqslant$ 5 MHz	$\pm$10	$\pm$97.7

The positioning methods were evaluated by FDD LTE link level simulations. The test scenarios follow 3GPP TS 36.133 [36]. Only one PRS occasion is used, thus the so-called prs-MutingInfo is set to 10000000 for all cells. One occasion has N_{PRS} subframes of data available, as shown in Table I. The prs-MutingInfo is a field specifying the PRS muting configuration of the cell [36]. The PRS muting configuration is defined by a periodic PRS muting sequence with periodicity T_{REP}, where T_{REP}, counted in the number of positioning occasions, can be 2, 4, 8, or 16, which is also the length of the selected bit string that represents this PRS muting sequence. If a bit in the PRS muting sequence is set to 0, then the PRS is muted in the corresponding PRS positioning occasion. For prs-MutingInfo set as 10000000, only the first occasion contains the PRS. A group of consecutive 1, 2, 4, or 6 subframes containing the PRS is referred to as a PRS positioning occasion. Different multipath channels, such as ETU, EVA, EPA and so on were taken to test non-LOS scenarios. Table III shows the details of simulation parameters, where two uncorrelated receive antennas were employed.

Three different methods for TOA/OTDOA estimation, namely, SNR threshold-based first tap detection (named as 'firstTap SNR'), adaptive threshold-based first tap detection (named as 'firstTap Adapt') and maximum/peak detection (named as 'maxPeak') were simulated. The 'maxPeak' can be considered as a state-of-the-art approach, as it is a direct outcome of the ML TOA estimation for AWGN channel (e.g. see [27]).

Table III. Simulation parameters.

Parameter	Value
Cell layout	2 cells
Cell ID set	[0, 3] [0, 6]
Network synchronisation	Synchronous
$\hat{E}$s/Noc set	[−6 dB, −13 dB]
Duplex mode	FDD
Cyclic prefix	Normal
DRX	OFF
Carrier frequency	2 GHz
Channel bandwidth	10, 5 and 1.4 MHz
Channel models	ETU, EPA,AWGN
UE speed	3 km/h, 5 km/h
PRS transmit antenna #	1
CRS transmit antenna #	2
Receive antenna #	2
Positioning subframes	no PDSCH in PRBs containing PRS
Positioning occasions	1
PRS pattern	6-reuse in frequency,
PRS power boosting	0 dB
PRS bandwidth	Full carrier bandwidth

The 90% percentile in cumulative distribution function (CDF) of the RSTD error, and 10%/90% percentile in CDF of the Rx–Tx time difference error are used to evaluate the accuracy of the OTDOA and TOA estimations, respectively. They are the parameters used to specify the 3GPP LTE positioning performance requirements. Note that 'maxPeak' selects the peak at discrete sample positions while the other two methods give the weighted sum of the first tap results, which leads to the step trend behaviour in 'maxPeak' method (Figures 7–15).

6.2. LTE RSTD measurement

Figure 7 shows the OTDOA measurement performances for AWGN channel with 10 MHz bandwidth, while the results for EPA5 channel are plotted in Figure 8. Dot-dashed green line denotes the 3GPP requirements. All three positioning methods fulfil the requirement. For AWGN, as well as EPA channel, the signal power is concentrated in the first arriving path, which can be simply located by selecting the peak/maximum of the correlation profile (e.g. using 'maxPeak'). Sometimes, the side lobe may be wrongly detected as the first arriving path by the 'firstTap SNR' method. The adaptive threshold-based detection has superior performance as its threshold changes with the noise and channel path power to reduce the side lobe effect.

Figure 9 shows the OTDOA measurement performances for ETU3 channel which, due to its large delay spread, belongs to the most critical channel profiles. The adaptive threshold-based method has the best performance among all, while the peak detection shows the worst performance.

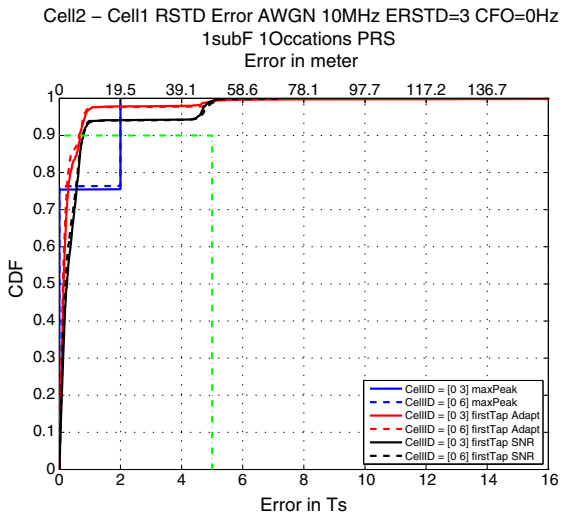

Figure 7. RSTD error statistics when using PRS (AWGN, 10 MHz LTE), where the dot-dashed green line shows the 3GPP requirement.

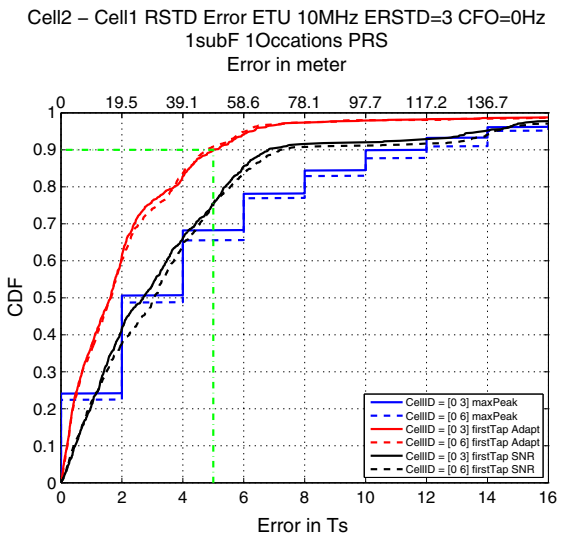

Figure 9. RSTD error statistics when using PRS (ETU3, 10 MHz LTE).

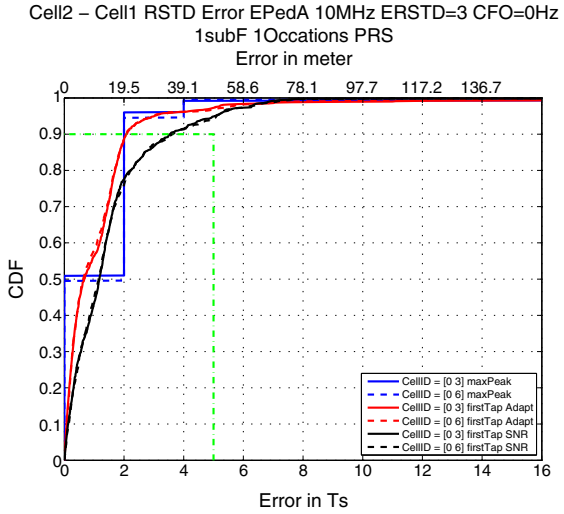

Figure 8. RSTD error statistics when using PRS (EPA5, 10 MHz LTE).

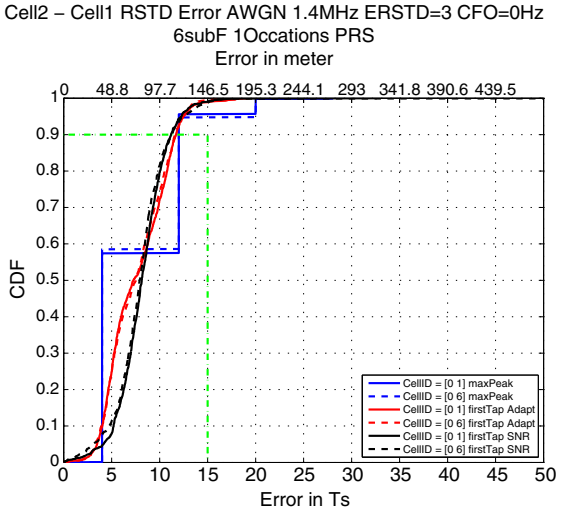

Figure 10. RSTD error statistics when using PRS (AWGN, 1.4 MHz LTE).

Because for an ETU channel, the first path is not the strongest channel path, the peak detection often leads to incorrect TOA estimation. Notice that the 3GPP EPA and ETU channel profiles have the root mean square delay spread of 45 and 991 ns, and the maximum excess tap delay of 410 and 5000 ns, respectively (see [33], section B.2).

Performances for the 1.4 MHz LTE are illustrated in Figures 10, 11 and 12. As for 1.4 MHz baseband signal, most of the channel paths are concentrated in the first arriving path, the first arriving path detection method tends to become peak detection. The neighbourhood smoothing and interpolation can further improve the estimation accuracy, so that the 3GPP requirements can be met in both AWGN and ETU channels.

One of the most critical test cases encountered in our investigations was ETU3 (Figure 9, Tables IV and V). As can be seen, for channels with a short delay spread (such as AWGN and EPA), all three methods work well, and the 3GPP requirements can be fulfilled. But for channels with a long delay spread (e.g. ETU), the method 'firstTap Adapt' works very robustly, followed by the 'firstTap SNR', whereas the peak detection based 'maxPeak' does not work anymore. Among the three investigated methods, only the 'firstTap Adapt' and using the PRS can meet the 3GPP requirements when no carrier frequency offset (CFO) is present. By using both PRS and CRS together, the 'firstTap Adapt' can in most cases fulfil the 3GPP requirements for a CFO of up to 400 Hz. CFO is usually caused

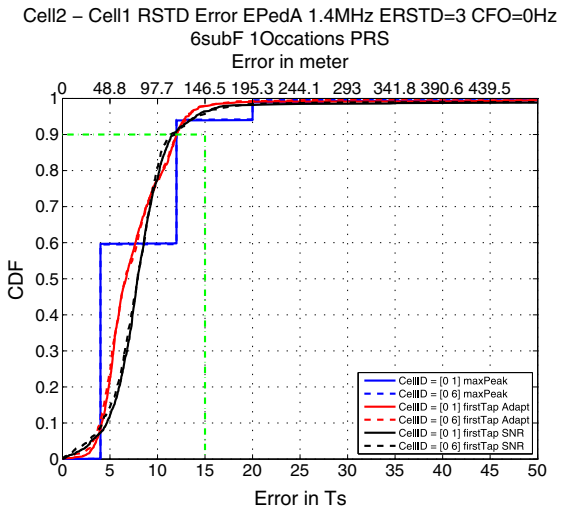

Figure 11. RSTD error statistics when using PRS (EPA5, 1.4 MHz LTE).

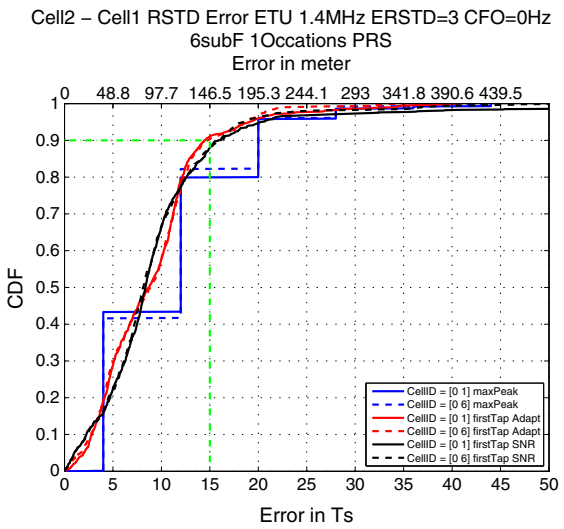

Figure 12. RSTD error statistics when using PRS (ETU3, 1.4 MHz LTE).

by the UE oscillator. By employing proper CFO estimation and compensation, the CFO can be controlled within 100 Hz (see, e.g. [37]), so that the 3GPP requirements can be met by the 'firstTap Adapt' even if relatively large CFO exists.

Simulations were also conducted using *only* the CRS. For an ETU channel, all three positioning methods investigated fail to meet the 3GPP requirements. For AWGN, all three methods fulfil the 3GPP Rel. 9 requirements, for LTE with 1.4 MHz till 20 MHz bandwidth, even if only CRS is used.

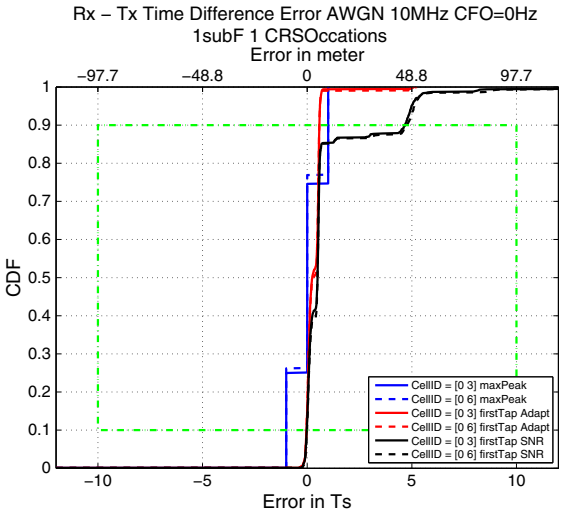

Figure 13. Rx–Tx time difference error statistics when using CRS (AWGN, 10 MHz LTE).

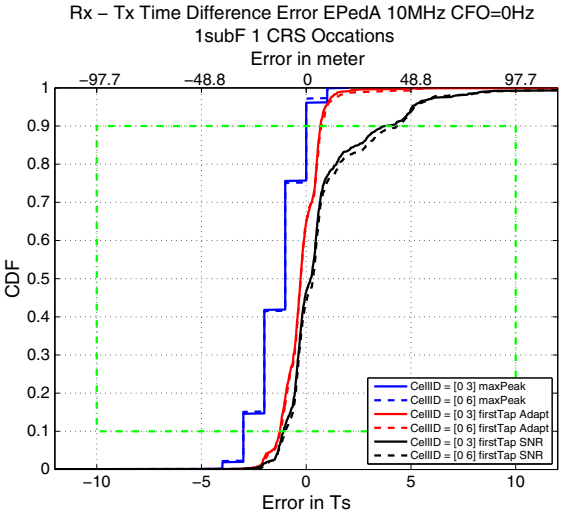

Figure 14. Rx–Tx time difference error statistics when using CRS (EPA5, 10 MHz LTE).

6.3. LTE Rx–Tx time difference measurement

Simulations with AWGN and ETU3 channel with SNR $=$ -6 dB were performed. Figures 13, 14, 15 and Table VI show some representative simulation results. All methods show good performance for AWGN. For ETU3 channel, both 'firstTap SNR' and 'firstTap Adapt' methods show their advantage in identifying the first tap. Further simulations show that the 'firstTap Adapt' performs best among the three methods and has a big margin to the 3GPP requirements.

Table IV. 90% RSTD error and the CRLB (in metre) using PRS. The data representing the best performances and fulfilling the 3GPP requirements are marked as **bold**, and the data not fulfilling the 3GPP requirements as *italic*.

		Bandwidth	1.4 MHz		5 MHz		10 MHz	
		$\sigma_{CRLB,90\%}$ for AWGN	17.8		3.7		1.8	
Method	Channel	CFO(Hz)\Cell ID	[0 1]	[0 6]	[0 3]	[0 6]	[0 3]	[0 6]
maxPeak	AWGN	0	117.2	117.2	39.1	39.1	19.5	19.5
		400	117.2	117.2	39.0	39.1	19.5	19.5
	EPA5	0	117.2	117.2	39.1	39.1	**19.5**	**19.5**
		400	**117.2**	**117.2**	39.0	39.1	**19.5**	**19.5**
	ETU3	0	*195.3*	*195.3*	*78.1*	*117.2*	*117.2*	*117.2*
		400	*195.3*	*195.3*	*117.2*	*117.2*	*117.2*	*136.7*
firstTap Adapt	AWGN	0	114.2	113.2	**12.1**	**12.0**	**6.6**	**6.3**
		400	116.2	111.2	13.6	13.4	**6.6**	**6.6**
	EPA5	0	117.2	117.5	22.7	21.7	20.2	20.3
		400	126.3	121.6	24.7	22.6	23.1	22.1
	ETU3	0	**140.8**	**143.8**	**42.5**	**43.4**	**48.2**	**47.0**
		400	**117.0**	*174.8*	**48.6**	**45.8**	*55.2*	*56.2*
firstTap SNR	AWGN	0	**109.3**	**110.2**	12.3	12.0	7.6	7.5
		400	**111.2**	**108.0**	**12.2**	**12.3**	22.1	44.8
	EPA5	0	**115.3**	**110.7**	**19.2**	**19.5**	34.5	35.5
		400	126.7	122.1	**19.3**	**18.3**	26.5	27.3
	ETU3	0	*154.7*	*156.5*	*64.4*	*75.8*	*66.5*	*70.2*
		400	*185.6*	*189.5*	*70.1*	*81.8*	*114.1*	*128.9*

Table V. 90% RSTD error and the CRLB (in metre) using PRS and CRS. The data representing the best performances and fulfilling the 3GPP requirements are marked as **bold**, and the data not fulfilling the 3GPP requirements as *italic*.

		Bandwidth	1.4 MHz		5 MHz		10 MHz	
		$\sigma_{CRLB,90\%}$ for AWGN	14.5		3.0		1.5	
Method	Channel	CFO(Hz)\Cell ID	[0 1]	[0 6]	[0 3]	[0 6]	[0 3]	[0 6]
maxPeak	AWGN	0	117.2	117.2	39.1	39.1	19.5	19.5
		400	117.2	117.2	39.1	39.1	19.5	19.5
	EPA5	0	117.2	117.2	39.1	39.1	**19.5**	**19.5**
		400	117.2	117.2	39.1	39.1	**19.5**	**19.5**
	ETU3	0	*195.3*	*195.3*	*78.1*	*117.2*	*117.2*	*117.2*
		400	*195.3*	*195.3*	*78.1*	*117.2*	*117.2*	*117.2*
firstTap Adapt	AWGN	0	107.7	105.7	**6.9**	**4.9**	**3.1**	**2.3**
		400	110.1	110.1	11.9	12.4	**4.8**	**5.8**
	EPA5	0	111.7	109.8	22.1	20.0	19.8	19.8
		400	117.6	114.9	23.5	21.2	20.9	20.6
	ETU3	0	**132.0**	**134.8**	**39.9**	**39.6**	**43.4**	**42.3**
		400	**141.8**	*155.3*	**44.4**	**43.3**	*49.1*	**47.4**
firstTap SNR	AWGN	0	**101.8**	**100.3**	11.9	11.2	6.8	6.5
		400	**105.0**	**105.8**	**11.3**	**11.1**	6.9	7.4
	EPA5	0	**104.8**	**103.6**	**18.4**	**18.3**	30.4	30.9
		400	**112.2**	**110.4**	**16.5**	**16.0**	24.4	26.0
	ETU3	0	143.2	*149.0*	54.8	*70.0*	*83.3*	*68.6*
		400	*154.2*	*163.2*	*60.7*	*72.8*	*116.2*	*117.0*

DOI: 10.1002/ett

Table VI. 10% and 90% Rx–Tx time difference error and the CRLB (in metre) using CRS. The data representing the best performances and fulfilling the 3GPP requirements are marked as **bold**, and the data not fulfilling the 3GPP requirements as *italic*.

		Bandwidth	1.4 MHz		5 MHz		10 MHz	
		$\sigma_{CRLB,90\%}$ for AWGN	10.3		2.1		1.1	
Method	Channel	CFO(Hz)\Cell ID	[0 1]	[0 6]	[0 3]	[0 6]	[0 3]	[0 6]
maxPeak	AWGN	0	**−117.2∼0.0**	**−117.2∼0.0**	−19.5∼19.5	−19.5∼19.5	−9.8∼9.8	−9.8∼9.8
		400	−117.2∼0.0	−117.2∼0.0	−19.5∼19.5	−19.5∼19.5	−9.8∼9.8	−9.8∼9.8
	EPA5	0	**−117.2∼0.0**	**−136.7∼0.0**	**−19.5∼0.0**	**−19.5∼0.0**	−29.3∼0.0	−29.3∼0.0
		400	**−117.2∼0.0**	**−136.7∼0.0**	**−19.5∼0.0**	**−19.5∼0.0**	−29.3∼0.0	−29.3∼0.0
	ETU3	0	−136.7∼78.1	−136.7∼58.6	−78.1∼−19.5	−78.1∼−19.5	*−146.5∼9.8*	*−136.7∼9.8*
		400	−136.7∼78.1	−136.7∼78.1	−78.1∼−19.5	−78.1∼−19.5	*−146.5∼−9.8*	*−136.7∼−9.8*
firstTap Adapt	AWGN	0	−127.1∼3.2	−128.0∼2.7	−0.4∼11.4	−0.3∼11.2	**−0.4∼5.7**	**−0.3∼5.7**
		400	−126.1∼4.8	−126.8∼2.9	**−0.8∼12.6**	**−0.9∼12.4**	**−0.4∼5.8**	**−0.4∼5.7**
	EPA5	0	−131.8∼−19.3	−132.4∼-21.1	−11.1∼11.7	−11.0∼11.1	**−12.3∼6.6**	**−12.1∼7.1**
		400	−131.1∼0.3	−130.7∼-16.3	−11.5∼12.4	−11.3∼11.5	**−13.2∼7.0**	**−13.3∼7.8**
	ETU3	0	**−119.5∼13.9**	**−123.1∼13.9**	**−39.5∼0.3**	**−38.7∼1.4**	−36.0∼5.8	−37.8∼5.1
		400	**−124.8∼14.9**	**−123.2∼15.3**	**−39.4∼2.7**	**−39.2∼3.5**	−41.5∼5.5	−44.8∼4.8
firstTap SNR	AWGN	0	−110.3∼15.5	−111.9∼13.5	**−0.4∼11.3**	**−0.5∼11.2**	**−0.2∼45.7**	**−0.1∼46.8**
		400	**−107.3∼18.7**	**−109.3∼16.8**	−2.3∼12.1	−2.0∼12.0	−0.1∼47.1	−0.2∼47.3
	EPA5	0	−116.4∼8.2	−116.2∼5.5	−12.4∼10.0	−12.2∼9.9	−10.7∼37.2	−9.8∼42.5
		400	−113.2∼15.7	−113.7∼10.3	−13.4∼6.3	−13.4∼5.3	−12.3∼13.7	−12.5∼11.6
	ETU3	0	−107.5∼37.8	−105.6∼38.0	−63.2∼−11.1	−62.0∼−10.0	**−32.0∼6.6**	**−33.4∼6.1**
		400	−113.2∼41.4	−116.1∼40.3	−68.3∼−13.6	−68.9∼−13.5	−48.5∼5.0	−49.3∼4.5

Trans. Emerging Tel. Tech. (2014) © 2014 John Wiley & Sons, Ltd.
DOI: 10.1002/ett

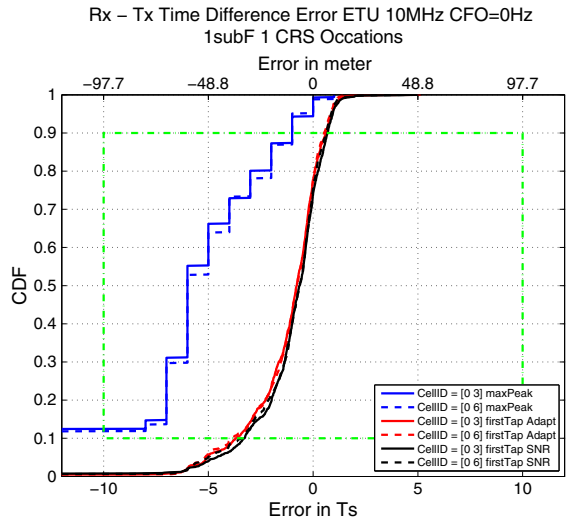

Figure 15. Rx–Tx time difference error statistics when using CRS (ETU3, 10 MHz LTE).

6.4. Some remarks

(1) *CRLB and practical LTE positioning:* From Table IV, V and VI, we see that the method based on first tap detection ('firstTap Adapt') achieves the best performances in most cases. For AWGN and high system bandwidth (e.g. 10 MHz in Table V), it can achieve a performance close to the corresponding CRLB. For low system bandwidth or for other mobile channels, there is, as expected, a significant gap between the performances of all three methods investigated and the CRLB of the static AWGN.

(2) *Impact of channel fading induced by multipath/shadowing:* We consider three representative mobile channels with different fading characteristics, namely, AWGN (no fading), EPA5 (weak fading due to small delay spread) and ETU (strong fading due to large delay spread). We take the most robust 'firstTap Adapt' method and the 10 MHz bandwidth as an example. For the 3GPP required RSTD error of 5 T_s, we obtain a CDF $=\sim$100% for AWGN (Figure 7), $\sim$97% for EPA5 (Figure 8) and $\sim$90% for ETU3 (Figure 9). In other words, to meet the same 3GPP accuracy requirement, the coverage of the estimator is reduced from 100% (without fading) to 97% for weak fading, and to 90% for strong fading. To be more specific, let us consider Table V, the 10 MHz case without CFO. To achieve the 90% coverage, the accuracy of the 'firstTap Adapt' estimate is degraded from $\sim$3 m for AWGN, to $\sim$20 m for EPA5, and further to $\sim$43 m for ETU3. Similar observations can be made for the other bandwidths as well as TOA estimation (Table VI). The impact of the channel variation on other two methods is still higher. As such, channel fading has a significant impact on the estimator performances and needs to be carefully addressed.

(3) *3GPP vs FCC requirements:* As can be seen from the aforementioned simulation results and analysis, the adaptive threshold-based approach can fulfil all 3GPP accuracy requirements for TOA and TDOA measurements under different multipath channels. It should be noted that for LTE bandwidths lower than or equal to 3 MHz, 3GPP requires an accuracy of 15 T_s for RSTD measurement, and an accuracy of 20 T_s for Rx–Tx time difference measurement, respectively (Table I and II). Roughly, 15 T_s corresponds to 150 m pseudo-range. For Gaussian-distributed measurement errors, the 150 m accuracy at the confidence level of 90% roughly corresponds to $150/1.64 =$ 91 m accuracy at the confidence level of 68%. Apparently, this accuracy does not meet the FCC requirement of 50 m at the confidence level of 67%. In other words, for bandwidths lower than or equal to 3 MHz, an LTE system even if it fulfils the 3GPP requirements (Rel. 9) may not necessarily meet the FCC requirement in terms of the positioning accuracy. Specifically, this can happen in some worst case scenarios such as the 1.4 MHz bandwidth for the channel ETU3 (see, e.g. Figure 12). According to our simulations, however, the FCC requirement can still be met in practice, for example, by averaging over multiple measurements, say, within a few seconds.

(4) *3GPP TOA and OTDOA tests:* 3GPP defines the requirements for the LTE TOA and OTDOA (Rel. 9) measurements in the core specification 36.133 for all practical channels (AWGN, multipath channel, etc.) [36]. However, the corresponding mandatory 3GPP TOA and OTDOA accuracy tests are up to now limited to the AWGN channel. As shown in our study, when only the AWGN is considered, all 3GPP LTE TOA and OTDOA accuracy requirements can be easily fulfilled, even using the simple peak detectionİ and using the CRS alone. Although the TOA and OTDOA accuracy tests under multipath channels are manufacturer specific, high accuracy positioning in this case is vital, as in real field the UE works in a multipath environment anyway.

(5) *Future LTE-A and 5th generation (5G) mobile systems:* The activities for the future 3GPP Rel. 12 to further enhance/tighten the positioning accuracy are ongoing (see, e.g. [38]). For 5G mobile systems, positioning accuracy below 0.5 m is required for some scenarios (see, e.g. [39]), which will be difficult to achieve with the current LTE-A positioning technique.

7. CONCLUSION

In this paper, we computed the CRLB of the LTE TOA and TDOA measurements using the different pilots, and analysed the achievable performance of the LTE system w.r.t. the FCC and 3GPP requirements and the impact of

multipath channels on the measurements. Then, we systematically investigated the 3GPP LTE TOA and OTDOA estimation using first arriving path detection. The proposed SNR-based threshold and adaptive threshold can both be used to detect the first path above it. Simulations showed that for multipath channels, the first arriving path detection leads to significantly better performance than the peak detection. Among the investigated methods, the adaptive threshold-based method showed the most robust performance and can fulfil all 3GPP LTE RSTD and Rx–Tx time difference measurement requirements, not only under AWGN but also under multipath (such as ETU3 at SNR $= -13$ dB) channels. It has low complexity, and for AWGN-like channel, it can sometimes achieve a performance close to the CRLB.

REFERENCES

1. Federal Communications Commission (FCC). *FCC 99-245. Third Report and Order*, Washington, DC, October 1999. Available from: http://www.fcc.gov/pshs/services/911-services/ [last accessed 6 October 1999].
2. Roxin A, Gaber J, Wack M, Nait-Sidi-Moh A. Survey of wireless geolocation techniques. In *IEEE Globecom Workshops*, Washington, DC, 2007; 1–9.
3. Zhao Y. Standardization of mobile phone positioning for 3G systems. *IEEE Communications Magazine* 2002; **40**(7): 108–116.
4. Pahlavan K, Li X, Makela J. Indoor geolocation science and technology. *IEEE Communications Magazine* 2002; **40**(2): 112–118.
5. Li X, Pahlavan K. Super-resolution TOA estimation with diversity for indoor geolocation. *IEEE Transactions on Wireless Communications* 2004; **3**(1): 224–234.
6. Prabhu V, Jalihal D. An improved ESPRIT based time-of-arrival estimation algorithm for vehicular OFDM systems. In *VTC'99 Spring*, Barcelona, 2009; 1–4.
7. Iannello JP. Time delay estimation via cross-correlation in the presence of large estimation errors. *IEEE Transactions on Acoustics Speech and Signal Processing* 1982; **30**: 998–1003.
8. Saarnisaari H. ML time delay estimation in a multipath channel. In *IEEE International Symposium on Software Testing and Analysis (ISSTA)*, San Diego, CA, USA, 1996; 1007–1011.
9. Zhang J, Kennedy RA, Abhayapala TD. Cramer-Rao lower bounds for the synchronization of UWB signals. *EURASIP Journal on Wireless Communications and Networking* 2005; **3**: 426–438.
10. Falsi C, Dardari D, Mucchi L, Win MZ. Time of arrival estimation for UWB localizers in realistic environments. *EURASIP Journal on Applied Signal Processing* 2006; **2006**: 1–13.
11. Wang D, Fattouche M. OFDM transmission for time-based range estimation. *IEEE Signal Processing Letters* 2010; **17**(6): 571–574.
12. Wang T, Shen Y, Mazuelas S, Win MZ. Bounds for OFDM ranging accuracy in multipath channels. In *Proceedings of IEEE International Conference on Ultra-Wideband (ICUWB)*, Bologna, Italy, 2011; 450–454.
13. Olenko AY, Wong KT, Qasmi SA. Distribution of the uplink multipaths' arrival delay and azimuth-elevation arrival angle because of 'bad urban' scatterers distributed cylindrically above the mobile. *Transactions on Emerging Telecommunications Technologies* 2013; **24**(2): 113–132.
14. Raulefs R, Zhang S, Mensing C. Bound-based spectrum allocation for cooperative positioning. *Transactions on Emerging Telecommunications Technologies* 2013; **24**(1): 69–83.
15. Xie Y, Wang Y, Wu B, You X. Mobile localisation with TOA, AOA and Doppler estimation in NLOS environments. *Transactions on Emerging Telecommunications Technologies* 2012; **23**(6): 499–507.
16. Laaraiedh M, Avrillon S, Uguen B. Cramer-Rao lower bounds for nonhybrid and hybrid localisation techniques in wireless networks. *Transactions on Emerging Telecommunications Technologies* 2012; **23**(3): 268–280.
17. Dardari D, Conti A, Ferner U, Giorgetti A, Win MZ. Ranging with ultrawide bandwidth signals in multipath environments. *Proceedings of IEEE* 2009; **97**(2): 404–426.
18. Dammann A, Mensing C, Sand S. On the benefit of location and channel state information for synchronization in 3GPP-LTE. In *European Wireless Conference (EW)*, Lucca, Italy, 2010; 711–717.
19. Zhu C. High accuracy multi-link synchronization in LTE: applications in localization. In *16th IEEE Mediterranean Electrotechnical Conference (MELECON)*, Tunisia, 2012; 908–913.
20. Medbo J, Siomina I, Kangas A, Furuskog J. Propagation channel impact on LTE positioning accuracy: A study based on real measurements of observed time difference of arrival. In *IEEE PIMRC*, Tokyo, Japan, 2009; 2213–2217.
21. Yang J, Wang X, Park S, Kim H. A novel first arriving path detection algorithm using multipath interference cancellation in indoor environments. In *IEEE VTC'10 Fall*, Ottawa, ON, 2010; 1–5.
22. 3GPP R4-100098. Link simulation results on OTDOA RSTD accuracy. In *Ericsson, ST-Ericsson*, Sophia Antipolis, France, 2010; 1–5.
23. 3GPP TS 36.211 Rel. 9. Evolved Universal Terrestrial Radio Access (E-UTRA); physical channels and

modulation. In *3rd Generation Partnership Project (3GPP)*, 2010.

24. Berkmann J, Carbonelli C, Dietrich F, Drewes C, Xu W. On 3G LTE terminal implementation - Standard, algorithms, complexities and challenges (Invited Paper). In *IEEE International Wireless Communications and Mobile Computing Conference (IWCMC)*, Crete, Greece, 2008; 970–975.
25. 3GPP TS 36.305 Rel. 9. Evolved Universal Terrestrial Radio Access Network (E-UTRAN); stage 2 functional specification of user equipment (UE) positioning in E-UTRAN. In *3rd Generation Partnership Project (3GPP)*, 2011.
26. 3GPP TS 36.214 Rel. 9. Evolved Universal Terrestrial Radio Access (E-UTRA); physical layer measurements. In *3rd Generation Partnership Project (3GPP)*, 2010.
27. Kay SM. *Fundamentals of Statistical Signal Processing: Estimation theory*. Prentice Hall, 1993.
28. Zanier F, Luise M. A new look into the issue of the Cramer-Rao bound for delay estimation of digitally modulated signals. In *IEEE ICASSP*, Taipei, Taiwan, 2009; 3313–3316.
29. Emmanuele A, Luise M, Won JH, Fontanella D, Paonni M, Eissfeller B, Zanier F, Lopez-Risueno G. Evaluation of filtered multitone (FMT) technology for future satellite navigation use. In *ION GNSS*, Portland, OR, 2011; 3743–3755.
30. Dammann A, Staudinger E, Sand S, Gentner C. Joint GNSS and 3GPP-LTE based positioning in outdoor-to-indoor environments - Performance evaluation and verification. In *24th International Technical Meeting of The Satellite Division of the Institute of Navigation (ION GNSS 2011)*, Portland, Oregon, USA, 2011; 3587–3595.
31. Del Peral-Rosado JA, Lopez-Salcedo JA, Seco-Granados G, Zanier F, Crisci M. Achievable localization accuracy of the positioning reference signal of 3GPP LTE. In *International Conference on Localization and GNSS (ICL-GNSS)*, Starnberg, 2012; 1–6.
32. Del Peral-Rosado JA, Lopez-Salcedo JA, Seco-Granados G, Zanier F, Crisci M. Joint channel and time delay estimation for LTE positioning reference signals. In *6th ESA Workshop on Satellite Navigation Technologies and European Workshop on GNSS Signals and Signal Processing (NAVITEC)*, Noordwijk, 2012; 1–8.
33. 3GPP TS 36.101 Rel. 9. Evolved Universal Terrestrial Radio Access (E-UTRA); user equipment (UE) radio transmission and reception. In *3rd Generation Partnership Project (3GPP)*, 2013.
34. Karisan Y, Dardari D, Gezici S, D'Amico AA, Mengali U. Range estimation in multicarrier systems in the presence of interference: performance limits and optimal signal design. *IEEE Transactions on Wireless Communications* 2011; **10**(10): 3321–3331.
35. Massey J. Optimum frame synchronization. *IEEE Transactions on Communications* 1972; **20**(2): 115–119.
36. 3GPP TS 36.133 Rel. 9. Evolved Universal Terrestrial Radio Access (E-UTRA); requirements for support of radio resource management. In *3rd Generation Partnership Project (3GPP)*, 2012.
37. Guo K, Xu W, Zhou G. Differential carrier frequency offset and sampling frequency offset estimation for 3GPP LTE. In *IEEE VTC'11 Spring*, Yokohama, Japan, 2011; 1–5.
38. 3GPP RP-130680. New SI proposal: positioning enhancements for E-UTRA (SI). In *Huawei et al*, 2013.
39. METIS, Mobile and wireless communications Enablers for the Twentytwenty Information Society, EU 7th Framework Programme project, 2014. D1.1 Scenarios, requirements and KPIs for 5G mobile and wireless system, Available from: http://www.metis2020.com/documents/deliverables/ [last accessed 30 April 2013].